Spontaneous Oscillations of Collective Molecular Motors

Frank Jülicher and Jacques Prost

Institut Curie, Physicochimie Curie, Section de Recherche, 26 rue d'Ulm, 75231 Paris Cedex 05, France
(Received 19 November 1996)

We present a physical mechanism which can lead to oscillatory motion of molecular motors cooperating in large groups when the system is elastically coupled to its environment. Analytical and numerical calculations reveal a characteristic type of oscillatory behavior with cusplike extrema. Typical oscillation frequencies are determined by the internal time scales of the motors. The physical mechanism we describe generates in a natural way many of the characteristic properties of spontaneous oscillations observed in some muscles and myofibrils. [S0031-9007(97)03323-1]

PACS numbers: 87.10.+e, 05.40.+j

Motor proteins are highly specialized macromolecules which can consume mechanical energy to induce motion and to generate forces. These molecules are involved in active transport processes, cell locomotion, and muscle contraction [1,2]. A typical motor molecule specifically attaches to a certain protein filament which serves as a track for its motion. In the presence of fuel, which in the cell is the molecule adenosine triphosphate (ATP), the motor starts moving in a direction defined by the polarity of the track. Experimental methods allow one to measure forces and velocities of individual motors or small groups of motors [3–7].

Normally, at given fuel concentration and temperature, motor molecules generate a constant average force leading to a constant average velocity [7]. In some cases, however, biological motors drive oscillatory motion: Insects move their wings back and forth with high frequency. While for some insects (e.g., butterflies) the timing of these oscillations is controlled by a periodic external nerve signal, others (e.g., bees and wasps) generate oscillations within the muscle [8]. Recently, spontaneous oscillations of single myofibrils (the contractile units of muscle cells) have been observed. These oscillations occur for certain well defined conditions of ADP and calcium concentrations, although *in vivo* these myofibrils are not designed to oscillate [9]. Since no oscillations of calcium concentration are detected, it seems reasonable to exclude a chemical origin for this behavior [8,9].

The purpose of this article is to describe theoretically a physical mechanism which allows for oscillatory motion of motor collections. Using both an analytical approach and a numerical study of a simple model, we show that motor collections acting on an elastic element quite generally have the potential to exhibit a periodic motion of a characteristic type without the need of a chemical oscillator. Furthermore, our model explains in a natural way the frequency range and the shape of the oscillations observed for myofibrils.

The microscopic mechanisms which are responsible for the force generation of biological motors are quite involved. In order to identify the main features of force generation and motion of molecular motors, simple physical models have been suggested [10–17]. One idea [11] is to simplify the internal degrees of freedom of the motor to two different states of a particle which moves along a one-dimensional coordinate x. The interaction of the particle with the track is described by potentials which reflect the periodic structure along the surface of the track. Within such a two-state model, motion is induced if the potentials are asymmetric with respect to $x \rightarrow -x$ (which reflects the polarity of the track) and if detailed balance of the transitions between states is broken [11]. Although the details of the behavior of biological motors are certainly far more complex, we think that the essential features of their motion are captured.

Additional phenomena occur if the collective motion of many particles is considered [18–20]. In a simple model, which mimics the way motors are coupled in muscles as well as experimental systems called "motility assays," particles are rigidly coupled to a common structure which they set in motion collectively [19,21] (see Fig. 1). As
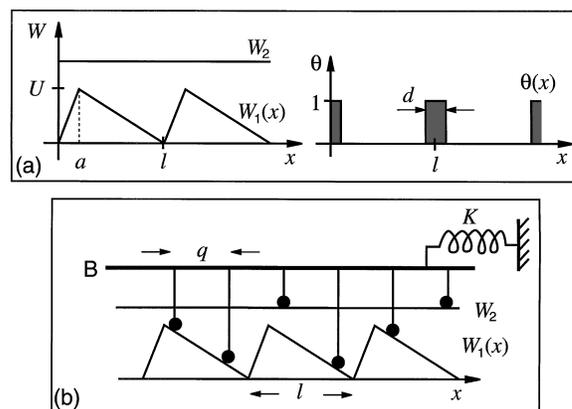

FIG. 1. (a) Periodic potentials W_1 and W_2 used to calculate the behavior of the system. The results presented in this article do not depend on the particular shape chosen. The function $\theta(x)$ is chosen to be nonzero in the vicinity of the potential minimum. (b) Many particles coupled rigidly to a backbone which is connected with its environment via a spring K. The particle spacing is denoted q.

a result of cooperation, motion can occur even in a symmetric system via spontaneous symmetry breaking. Related instabilities occur also in asymmetric systems, revealing the rich behavior of many-motor systems.

In the following, we demonstrate that many coupled motors can induce instabilities towards a state with periodically varying velocity. Such instabilities occur if the system is elastically coupled to its environment. Note that such a situation occurs naturally in most realistic cases. For example, in muscles, the spring of Fig. 1 represents the elastic properties of structures which connect the active elements [1,22].

In order to model many-motor systems, it is essential to start with a simple description of individual motors. We therefore consider the two-state models mentioned above where motors are represented by particles which move in two periodic potentials $W_\sigma(x)$ with period l. Transitions between states $\sigma = 1, 2$ occur with l-periodic rates $\omega_1(x)$ and $\omega_2(x)$. The excitation amplitude can be written as [11] $\omega_1(x) = \omega_2(x)[\exp[(W_1 - W_2)/T] + \Omega\theta(x)]$, where T denotes temperature measured in units of the Boltzmann constant. We assume that the periodic function $\theta(x)$ is given. In principle it can be calculated from a specific model for the reaction kinetics of the fuel coupled to the particle [23]. The amplitude Ω describes the activity of the chemical fuel and measures the distance from thermal equilibrium.

We assume that the particles are rigidly connected to a common backbone with a fixed spacing q incommensurate with the potential period l [24]. This corresponds to the arrangement of motors along their track in muscles [2], but also to the disorder of motors in motility assays. In the limit of a large system one can introduce densities $P_\sigma(\xi)$ with $\sigma = 1, 2$ which give the probability to find a particle at position $\xi = x \bmod l$ relative to the beginning of the potential period in state σ. These densities are not independent but obey $P_1(\xi) + P_2(\xi) = 1/l$ and $\int_0^l d\xi(P_1 + P_2) = 1$. The equations of motion for this system read [19]

$$\partial_t P_1 + v\partial_\xi P_1 = -\omega_1 P_1 + \omega_2 P_2 ,$$
$$\partial_t P_2 + v\partial_\xi P_2 = \omega_1 P_1 - \omega_2 P_2 , \qquad (1)$$

$$f_{\text{ext}} = \lambda v + KX + \int_0^l d\xi P_1 \partial_\xi(W_1 - W_2) . \qquad (2)$$

Equation (1) describes the dynamics of the density $P_1(\xi)$ resulting from motion of the backbone with velocity $v = \partial_t X$ and the transitions between the states. Equation (2) is a force balance: The externally applied force per particle $f_{\text{ext}}(t)$ is balanced by friction with damping coefficient λ, by the average force due to the potentials and the additional elastic force KX of a spring of length X with elastic modulus KN where N is the number of particles. Note that Eqs. (1) and (2) depend only on the difference $W_1 - W_2$ of the two potentials, and we can choose W_2 to be constant without loss of generality.

As a consequence of the spring action, a nonmoving solution to Eqs. (1) and (2) with $v = 0$ exists for $f_{\text{ext}} = 0$, $P_1 = R \equiv \omega_2/(\alpha l)$, where $\alpha(\xi) \equiv \omega_1(\xi) + \omega_2(\xi)$ and $X = X_0 \equiv -\int_0^l d\xi R\partial_\xi(W_1 - W_2)/K$. We study the linear stability of this solution and determine the instability threshold with respect to oscillations. With the ansatz $P_1(\xi, t) = R(\xi) + p(\xi)\exp(st)$, $v(t) = u\exp(st)$, and $X(t) = X_0 + u\exp(st)/s$, one finds using Eqs. (1) and (2) to linear order in p and the velocity amplitude u: $p(\xi) = -u\partial_\xi R/[s + \alpha(\xi)]$. The possible values of the complex eigenvalue $s = -\tau + i\omega$ are determined by

$$\lambda + \frac{K}{s} = \int_0^l d\xi \frac{\partial_\xi R \ \partial_\xi(W_1 - W_2)}{s + \alpha(\xi)} . \qquad (3)$$

The nonmoving state is unstable if $\tau < 0$. The instability occurs for $\tau = 0$, where the real part of s vanishes. This happens at a threshold value $\Omega = \Omega_c(K)$ for which $\alpha(\xi) = \alpha_c(\xi)$. In the limit $K = 0$ where no elastic element is present, it follows from the imaginary part of Eq. (3) that $\omega_c = 0$. The real part then determines $\Omega_c(0)$, which is the condition for the instability of the nonmoving state as previously described in Ref. [19]. For nonzero K the instability occurs for $\Omega_c(K) = \Omega_c(0) + \delta\Omega_c$ with $\delta\Omega_c \sim K$ for small K, and the system starts to oscillate with finite angular frequency $\omega_c \sim K^{1/2}$. Note that beyond a maximal value $K > K_{\max}$, the resting state is stable for any value of Ω.

Figure 2 shows examples for these oscillations which have been calculated by numerically integrating Eqs. (1) and (2) for constant deexcitation rate ω_2 and piecewise linear potentials. The function $\theta(\xi)$ is chosen as shown in Fig. 1(a) with $d/l = 0.1$. Figure 2(a) displays the position X versus time t for an excitation level $\Omega = 0.1$ slightly above threshold. After an initial relaxation period, motion is almost sinusoidal. An example for small elastic modulus is shown in Fig. 2(b). This case corresponds to the nonlinear regime far away from the instability. It results from the existence of a hysteresis loop in the steady state force-velocity curve in the absence of an elastic element as described in [19]. The progressive loading of the spring allows one to follow the hysteresis loop: This is visible through the cusplike extrema of the filament position versus time [Figs. 2(b) and 2(c)]. The oscillations can be obtained both for symmetric and asymmetric potentials. The asymmetry directly reflects on the asymmetry of the $X(t)$ curve as a comparison of Figs. 2(b) and 2(c) shows.

In order to give additional insight into the properties of the system, we present an analytical description of oscillations in the vicinity of the instability. Anticipating that the motion is periodic with period $t_P \equiv 2\pi/\omega$, we can write $P_1(\xi, t) = \sum_{k=-\infty}^{\infty} P_1(\xi, k)e^{ik\omega t}$, $v(t) = \sum_{k=-\infty}^{\infty} v_k e^{ik\omega t}$, and $f_{\text{ext}}(t) = \sum_{k=-\infty}^{\infty} f_k e^{ik\omega t}$, which defines the Fourier coefficients $P_1(\xi, k)$, v_k, and f_k. Using this representation, one can derive the nonlinear relation
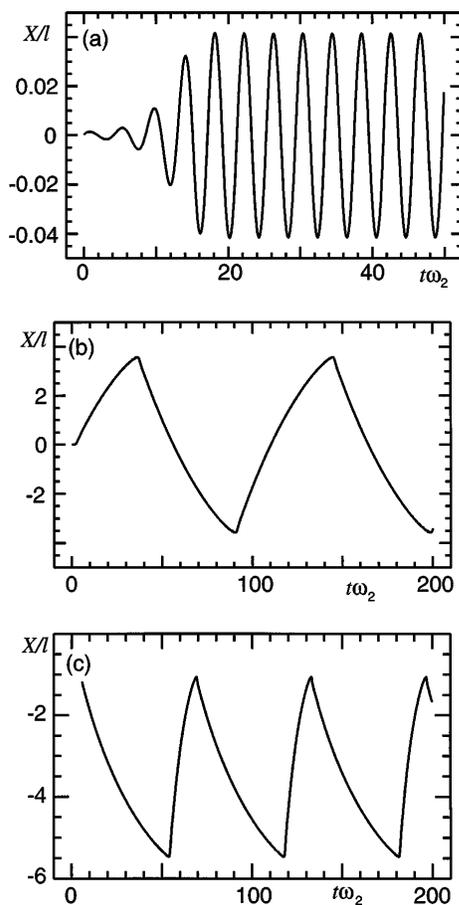
FIG. 2.　(a) Position X versus time t for a symmetric system with $a/l = 0.5$, $d/l = 0.1$,, $\Omega = 0.1$, $\lambda\omega_2 l^2/U = 0.1$, and $Kl^2/U = 0.2$.　(b) Same system but $Kl^2/U = 0.002$. Note that the oscillations have the symmetry property $X(t + t_P/2) = -X(t)$, where t_P is the temporal period.　(c) Oscillations for an asymmetric system with $a/l = 0.1$ for $Kl^2/U = 0.01$ and otherwise the same parameters as in (b). Note the similarity with the oscillation shape shown in Fig. 4 of Ref. [9].

between velocity and external force

$$f_k = F^{(1)}_{kl} v_l + F^{(2)}_{klm} v_l v_m + F^{(3)}_{klmn} v_l v_m v_n + O(v^4).$$

(4)

The coefficients $F^{(n)}_{k,k_1,\ldots,k_n}$ can be calculated by first rewriting Eq. (1) as

$$P_1(\xi, k) = \delta_{k,0} R(\xi) - \sum_{lm} \frac{\delta_{k,l+m}}{\alpha + i\omega k} v_l \partial_\xi P_1(\xi, m).$$

(5)

Inserting the ansatz

$$P_1(\xi, k) = R\delta_{k,0} + P^{(1)}_{kl}(\xi) v_l + P^{(2)}_{klm}(\xi) v_l v_m + O(v^3)$$

(6)

into Eq. (5), one obtains a recursion relation for the functions $P^{(n)}_{k,k_1,\ldots,k_n}$:

$$P^{(n)}(\xi)_{k,k_1,\ldots,k_n} = -\sum_l \frac{\delta_{k,k_n+l}}{\alpha + i\omega k} \partial_\xi P^{(n-1)}_{l,k_1,\ldots,k_{n-1}}.$$

(7)

Using Eq. (2), one finds

$$F^{(1)}_{kl} \equiv \delta_{kl}\left(\lambda + \frac{K}{i\omega k} - \int_0^l d\xi \frac{\partial_\xi R\partial_\xi[W_1 - W_2]}{\alpha + i\omega k}\right).$$

(8)

The linear response function of the system is given by the inverse of $F^{(1)}_{kl}$. Therefore the instability condition Eq. (3) corresponds to $F^{(1)}_{kl} = 0$. For $n > 1$,

$$F^{(n)}_{k,k_1,\ldots,k_n} \equiv \int_0^l d\xi P^{(n)}(\xi)_{k,k_1,\ldots,k_n} \partial_\xi(W_1 - W_2).$$

(9)

Note that the coefficients $F^{(n)}_{k,k_1,\ldots,k_n}$ are nonzero only if $k = k_1 + \cdots + k_n$. If no elastic coupling to the environment is present, i.e., $K = 0$, one recovers for constant external force f_0 the steady states which have been described previously [19]: $f_{\text{ext}} = f_0(v_0)$; $v_k = 0$ for $k \neq 0$. As soon as $K \neq 0$, v_0 must vanish and a constant external force f_0 only changes the average position X_0.

Spontaneous oscillations are solutions to Eq. (4) for $f_k = 0$ ($k \neq 0$). The dominant terms near the instability of v_1 are given by

$$0 = F^{(1)}_{11} v_1 + G^{(2)} v_{-1} v_2 + G^{(3)} v_1^2 v_{-1},$$

(10)

$$0 = F^{(1)}_{22} v_2 + F^{(2)}_{211} v_1^2,$$

(11)

where $G^{(2)} \equiv F^{(2)}_{1,2,-1} + F^{(2)}_{1,-1,2}$ and $G^{(3)} \equiv F^{(3)}_{1,1,1,-1} + F^{(3)}_{1,1,-1,1} + F^{(3)}_{1,-1,1,1}$. As soon as v_1 and v_2 are determined, higher orders v_k can be obtained recursively using Eq. (4). From Eq. (11) one finds that $v_2 \sim v_1^2$. Inserting this value in Eq. (10), one obtains $0 = F^{(1)}_{11} v_1 + \tilde{G}^{(3)} v_1^2 v_{-1}$, with an effective coefficient $\tilde{G}^{(3)} \equiv G^{(3)} - F^{(2)}_{211} G^{(2)}/F^{(1)}_{22}$. One solution is always $v_1 = 0$. The remaining solutions are described by $|v_1|^2 = -F^{(1)}_{11}/\tilde{G}^{(3)}$. Since the amplitude $|v_1|^2$ is a real number, while $F^{(1)}_{11}$ and $\tilde{G}^{(3)}$ are in general complex, solutions exist only for a unique oscillation frequency ω_s. Typical frequencies selected near the instability have values of the order of magnitude of the transition rate $\omega_s \sim \omega_2$.

The parameters used in Fig. 2 are close to typical physiological conditions valid for the actin/myosin case: potential period $l \simeq 10$ nm, energy scale $U \simeq 10 k_B T$, frequency scale $\omega_2 \simeq 10^3$ s^{-1}, and damping coefficient $\lambda \simeq 10^{-8}$ kg/s. The value of λ is a guess assuming a local viscosity 10^2 to 10^3 times larger than that of water. Oscillation frequencies in this case vary between $\omega_s = 0$ for $K = 0$ and $\omega_s \simeq 5\omega_2$ for $K \simeq K_{\max} \simeq 10^{-3}$ N/m per motor. This shows that using typical time scales of biological motors the mechanism described here generates naturally frequencies up to the kHz range, to be compared

with the known frequencies of insect flight muscles in the 100 Hz range [8].

Our model assumes an infinite number of particles for simplicity, and one has to estimate the minimum number of motors required for the existence of oscillations. Neglecting all fluctuations, this number is three. The effect of fluctuations, both thermal and stochastic, is to destroy the phase coherence of the oscillations but not the oscillation phenomenon itself. We estimate the coherence time to be bounded by $\omega_2^{-1} \exp(N)$, where N is the number of motors involved in the process. For a single filament in muscles, $N \simeq 300$ [1], so that the coherence time is large. In addition, these structures are connected three dimensionally, which reduces fluctuations even more. Another interesting estimate is the maximal length of a motor collection for which the approximation of rigid backbone remains valid. Its compressibility becomes important as soon as elastic deformations lead to length changes of the order of the potential period. Using the stretching elasticity of actin as an example for the material properties of protein filaments, one can calculate the Young's modulus using the persistence length of 15 μm, and the diameter of a few nm [25]. This estimate suggests that for typical lateral forces of several 10 pN our approximation is valid for filaments with a length of up to several μm, to be compared with the 2 μm length of muscle filaments.

In summary, we have shown using a simple two-state model that collections of motor molecules may spontaneously oscillate. Our results are fairly robust in that they neither depend on the particular choice of the potential shape, nor on the exact type of connection to the common backbone. They simply require that the transitions from state one to two are localized in "active sites" close to the energy minima. Our mechanism allows for oscillations in myofibrils and in insect muscles directly via the force generation. The particular type of oscillations which we predict show a shape which includes cusplike maxima and minima; see Figs. 2(b) and 2(c). It is striking to note that the observed oscillations of myofibrils exhibit the characteristic properties which we predict: The shape of the oscillations with cusplike extrema and oscillations nonaffected both in frequency and amplitude by a constant externally applied force [9].

[1] B. Alberts, D. Bray, J. Lewis, M. Raff, K. Roberts, and J. D. Watson, *The Molecular Biology of the Cell* (Garland, New York, 1994).

[2] H. E. Huxley, Science **164**, 1365 (1969).

[3] J. A. Spudich, Nature (London) **348**, 284 (1990).

[4] A. Ishijima, T. Doi, K. Sakurada, and T. Yanagida, Nature (London) **352**, 301 (1991).

[5] K. Svoboda, C. F. Schmidt, B. J. Schnapp, and S. M. Block, Nature (London) **365**, 721 (1993).

[6] A. J. Hunt, F. Gittes, and J. Howard, Biophys. J. **67**, 766 (1994).

[7] D. A. Winkelmann, L. Bourdieu, A. Ott, F. Kinose, and A. Libchaber, Biophys. J. **68**, 2444 (1995); L. Bourdieu, M. O. Magnasco, D. A. Winkelman, and A. Libchaber, Phys. Rev. E **52**, 6573 (1995).

[8] J. W. S. Pringle, in *Insect Flight Muscle,* edited by R. T. Tregear (North-Holland, Amsterdam, 1977), p. 177.

[9] K. Yasuda, Y. Shindo, and S. Ishiwata, Biophys. J. **70**, 1823 (1996).

[10] A. Ajdari and J. Prost, C. R. Acad. Sci. Ser. 2 **315**, 1635 (1992).

[11] J. Prost, J.-F. Chauwin, L. Peliti, and A. Ajdari, Phys. Rev. Lett. **72**, 2652 (1994); J.-F. Chauwin, A. Ajdari, and J. Prost, Europhys. Lett. **27**, 421 (1994).

[12] C. S. Peskin, G. B. Ermentrout, G. Oster, in *Cell Mechanics and Cellular Engineering,* edited by V. Mow *et al.* (Springer, New York, 1994).

[13] R. D. Astumian and M. Bier, Phys. Rev. Lett. **72**, 1766 (1994).

[14] M. O. Magnasco, Phys. Rev. Lett. **71**, 1477 (1993); **72**, 2656 (1994).

[15] C. R. Doering, Nuovo Cimento **17**, 685 (1995).

[16] I. Derényi and T. Vicsek, Proc. Nat. Acad. Sci. **93**, 6775 (1996).

[17] H. X. Zhou and Y. Chen, Phys. Rev. Lett. **77**, 194 (1996).

[18] S. Leibler and D. Huse, J. Cell Biol. **121**, 1357 (1993).

[19] F. Jülicher and J. Prost, Phys. Rev. Lett. **75**, 2618 (1995).

[20] I. Derényi and T. Vicsek, Phys. Rev. Lett. **75**, 374 (1995); I. Derenyi and A. Ajdari, Phys. Rev. E **54**, 5–8 (1996).

[21] Flexibility of motors could be modeled in two different ways: (i) By introducing springs between the particles and the rigid structure, and (ii) by keeping track of the backbone compressibility. We have checked that (i) does not alter the essential features discussed here. Case (ii) is irrelevant for sufficiently short filaments as we explain in the text.

[22] Note that at the microscopic length scales of the motors inertia is negligible and motion is overdamped. Our approach is therefore in contrast to models where inertia terms are needed to obtain oscillations; see, e.g., S. Scilia and D. A. Smith, Math. Biosci. **106**, 159 (1991).

[23] F. Jülicher, A. Ajdari, and J. Prost (to be published).

[24] This incommensurability is not essential for the collective effects which we describe here but represents the case for which calculations are most simple.

[25] F. Gittes, B. Mickey, J. Nettleton, and J. Howard, J. Cell. Biol. **120**, 923 (1993).